

Molecular Dynamics Simulation Studies of Self-Assembly of Racemic (*R*)/(*S*)-2-Bromohexadecanoic Acid on a Graphite Surface: Enantio-pure or Enantio-mixed Domains?

Boaz Ilan, B. J. Berne,* and George W. Flynn*

Department of Chemistry and Columbia Center for Electron Transport in Molecular Nanostructures,
Columbia University, New York, New York 10027

Received: July 19, 2007; In Final Form: September 25, 2007

The morphological enantio-identity of racemic (*R*)/(*S*)-2-bromohexadecanoic acid self-assemblies on graphite is examined according to molecular dynamics simulations of the optimized potential for liquid simulations (OPLS) force field. Racemic (*R*)/(*S*)-2-bromohexadecanoic acid segregates at the graphite–solvent interface into coexisting domains characterized by approximately 50° clockwise and 50° counter-clockwise lamellae-trough angles. The “upward” orientation (away from the graphite surface) of bromine atoms has been observed experimentally to be thermodynamically more stable under solvent for a wide range of bromo-substituted organic molecules, suggesting that the domains of racemic (*R*)/(*S*)-2-bromohexadecanoic acid observed by scanning tunneling microscopy under phenyl octane solvent consist of pure enantiomers. Our calculations, performed under vacuum conditions, suggest a competition between the stability gained by mixing “upward” and “downward” pairs of (*R*) and (*S*) enantiomers and the symmetry breaking that favors the “upward” orientation of the bromine atoms at the graphite–solvent interface. The calculations indicate that racemic (*R*)/(*S*)-2-bromohexadecanoic acid is likely to form enantio-mixed domains at the graphite–vacuum interface. The possibility that the domains formed by racemic (*R*)/(*S*)-2-bromohexadecanoic acid at the graphite–solvent interface are not enantio-pure is discussed in this paper.

Introduction

The specificity of nature toward chiral molecules such as helical DNA and L-amino acids is fundamental to biomolecular recognition and the preparation of optically active drugs, fragrances, and flavors. Chiral resolution, the process by which racemic compounds are separated into their enantiomers, can be achieved by several methods such as crystallization, chiral resolving agents, chiral column chromatography, and enantioselective surfaces. The latter can be created by chiral modifiers such as catalytic “kinks” of either left- or right-handed versions.¹ Heterogeneous catalytic surfaces are industrially very promising because they offer engineering flexibility, efficient catalytic recycling, and an impressive output of enantiomeric excess for certain reactions.² Surfaces are also fascinating mediums for the study of chirality in that they narrow the number of symmetry operations available to adsorbed molecules. Achiral molecules, for example, may form chiral domains on surfaces due to the loss of rotational and translational degrees of freedom.³ The supramolecular self-assembly of chiral molecules on surfaces has also been studied extensively in recent years.^{4–7}

Integral equation theories, as well as molecular dynamics and periodic density functional theory simulations, have been employed in the past^{8–11} to interpret the experimental self-assembly of chiral molecules at interfaces. These studies are beginning to provide theoretical guidelines that govern the importance of molecular shape, chiral asymmetry, and the balance of force field contributions (such as dispersion interactions and electrostatics) in determining chiral resolution. Such

guidelines are of considerable importance in designing experimental efforts to identify candidate catalytic surfaces for chiral resolution and candidate chiral molecules that can be used in “bottom-up” patterning of surfaces with desired symmetry properties. In this paper, we investigate theoretically the properties of supramolecular self-assembled morphologies of the chiral (*R*)/(*S*)-2-bromohexadecanoic acid molecule, CH₃(CH₂)₁₃CH(Br)COOH, on the highly oriented pyrolytic graphite (HOPG) surface.

The self-assembly of mixtures of (*R*)-2-bromohexadecanoic acid with hexadecanoic acid and (*S*)-2-bromohexadecanoic acid with hexadecanoic acid at the solvent–graphite (phenyloctane–graphite) interface has been studied using scanning tunneling microscopy (STM) techniques.¹² The pure enantiomers interperse sporadically within the template of a 90° lamellae-trough (LT) morphology formed by the inherently achiral hexadecanoic acid. They associate either with themselves (as pairs of (*R*) with (*R*) or (*S*) with (*S*)) or with other hexadecanoic acid molecules. The molecular modeling obtained¹² for such a pair of (*R*) enantiomers and a pair of (*S*) enantiomers is depicted in Figure 1A and B, respectively. The molecular model implies unambiguously that the bromine atoms point “up”, away from the graphite surface. The (*R*) pair and the (*S*) pair are mirror images of each other characterized by clockwise and counter-clockwise orientation of the hydrogen bond of the carboxylic groups, respectively. The up orientation of the bromine atoms is generally thermodynamically more stable as determined by systematic STM¹³ and theoretical¹⁴ studies of halogen-substituted organic molecules at the graphite–solvent interface.

The self-assembly of racemic mixtures of (*R*)/(*S*)-2-bromohexadecanoic acid has been studied at the phenyloctane–

* Authors to whom correspondence should be addressed: G.W. Flynn — Phone: 212-854-4162, E-mail: gwfl@columbia.edu; B.J. Berne — Phone: 212-854-2186, E-mail: bb8@columbia.edu.

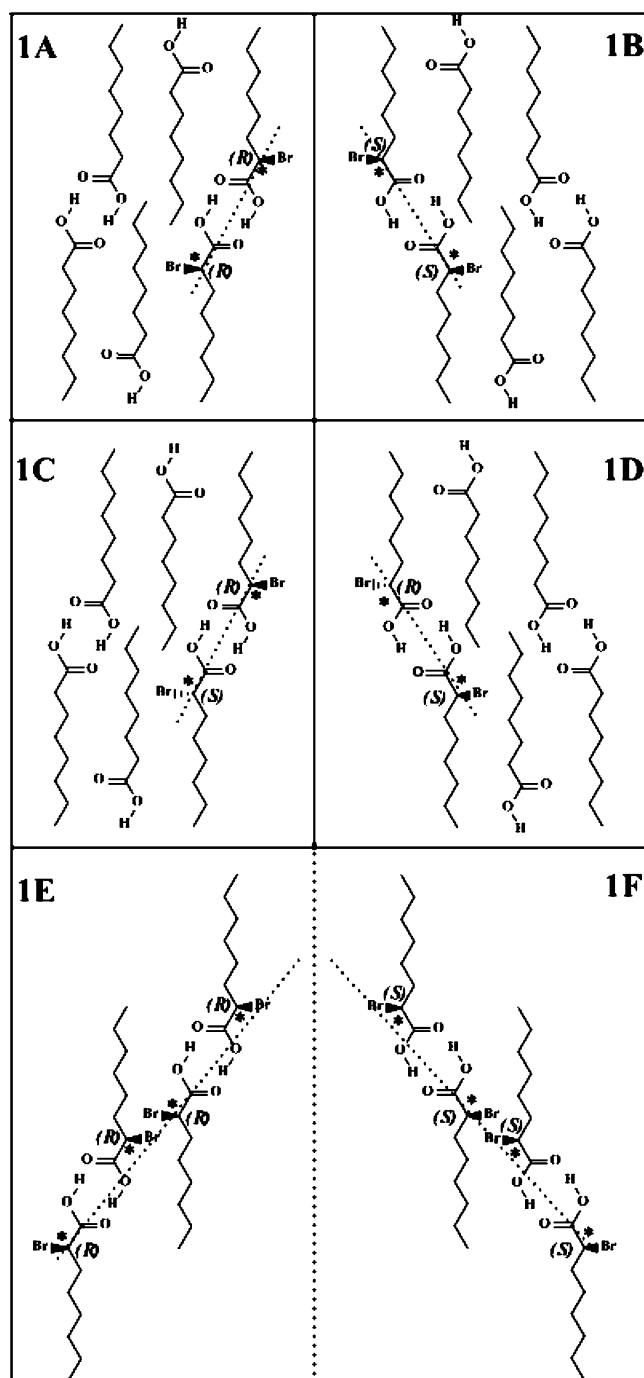


Figure 1. 1A and 1B depict schematic molecular models¹² of hexadecanoic acid coadsorbed with (*R*) and (*S*) enantiomers of 2-bromohexadecanoic acid, respectively. The tails of the chains have been truncated for illustration purposes. The enantiomers are sporadically interspersed within the 90° LT angle template of the hexadecanoic acid. The bromine atoms are unambiguously oriented up. 1C and 1D depict hypothetical molecular models of coadsorbate hexadecanoic acid with a racemic mixture of (*R*)/(*S*)-2-bromohexadecanoic acid for which the domains are enantio-mixed. The enantio-mixed pairs in 1C and 1D are *R*(u)/*S*(d) and *R*(d)/*S*(u), respectively. 1E and 1F depict hypothetical molecular models of enantio-pure domains formed by the self-assembly of racemic (*R*)/(*S*)-2-bromohexadecanoic acid (i.e., without coadsorbate). The bromine atoms are oriented up. The two domains are mirror images of each other across the reflection plane indicated by the vertical dashed line. The mirror symmetries are characterized by 50° clockwise and 50° counter-clockwise LT angles depicted by the diagonal dashed lines in 1E and 1F, respectively.

graphite interface both in the absence^{15,16} and in the presence¹⁷ of the coadsorbate hexadecanoic acid. Coadsorbed with hexa-

decanoic acid,¹⁷ the racemic mixture displays two distinct domains that appear (within the STM resolution) exactly like the morphologies observed for the (*R*) enantiomer with hexadecanoic acid, and the (*S*) enantiomer with hexadecanoic acid noted above. The domains range in width between 30 and 100 nm. They are likely to be enantio-pure only if the up orientation of the Br atoms is also favorable relative to the stability gained by mixing the enantiomers. The clockwise and counter-clockwise orientation of the hydrogen bond of the carboxylic groups could also be fitted, in principle, by molecular models of pairs of *R*(u)/*S*(d) (Figure 1C) and *R*(d)/*S*(u) (Figure 1D), respectively, where u stands for up and d stands for down. This situation is in contrast to the case discussed previously for the coadsorption of a pure enantiomer with hexadecanoic acid where the identity of the enantiomers is known a priori and the molecular model serves to unambiguously identify (according to the clockwise or counter-clockwise property of the hydrogen bonds) the orientation of the Br atoms as up. Racemic (*R*)/(*S*)-2-bromohexadecanoic acid does not crystallize in the bulk phase into a mixture of enantio-pure crystals,¹⁸ suggesting a competition between the driving force for the mixing of pairs of (*R*) and (*S*) enantiomers and the stability of the up orientation of the bromine atoms at the graphite–solvent interface.

The formation of domains consisting exclusively of either clockwise or counter-clockwise oriented carboxylic hydrogen bonds (dashed lines in Figure 1A and B) is perhaps surprising because the 2-bromohexadecanoic acid molecules are dilutely interspersed within the template morphology of the inherently achiral hexadecanoic acid. In fact, however, hexadecanoic acid forms two domains exhibiting non-superimposable mirror-image morphologies (enantiomorphous domains) when confined to the two-dimensional world of a graphite surface, a general feature observed for fatty acids possessing an even number of carbon atoms.¹⁹ The two domains are characterized by the clockwise and counter-clockwise orientations of the hydrogen bonds (see, for example, the orientation of the hydrogen bonds for the left-most and right-most pairs of hexadecanoic acid molecules in Figure 1A and B, respectively.) The 2-bromohexadecanoic acid molecules enable, therefore, the identification of the enantiomorphous domains of the hexadecanoic acid through the capacity of the Br atoms to serve as STM chemical markers.²⁰ The segregation of hexadecanoic acid into enantiomorphous domains also suggests the existence of domains entirely devoid of 2-bromohexadecanoic when coadsorbed with either of the pure enantiomers of 2-bromohexadecanoic acid (discussed above). Such domains should exist because morphologies containing “downward”-facing Br atoms (of 2-bromohexadecanoic acid) have not been observed.¹²

By itself, that is, without the coadsorbate hexadecanoic acid, racemic (*R*)/(*S*)-2-bromohexadecanoic acid forms coexisting domains at the phenyloctane–graphite interface ranging in width from 30 to 100 nm.^{15,16} The domain morphologies differ from the template morphologies (90° LT angle) of the hexadecanoic acid and are characterized by (approximately) 50° clockwise and 50° counter-clockwise LT angles (Figure 1E and F, respectively). The LT angle has been measured experimentally to be approximately 45° in ref 15 and approximately 53° in ref 16. The chains form alternating head-to-tail and tail-to-head columns, thereby maximizing the number of bromine–bromine interactions while maintaining the hydrogen bonds between pairs of carboxylic groups. The domains depicted schematically in Figure 1E and F are enantio-pure (Br atoms are oriented up). However, this need not necessarily be the case as discussed above (coadsorbate self-assembly). Should the balance of forces

tip toward enantiomeric mixing, then the domains would necessarily consist of mixtures of $R(u)/S(d)$ or $R(d)/S(u)$. The ordering within these domains is also not necessarily unique. For example, considering the $R(u)/S(d)$ domain, the ordering along the lamellae could be, in principle, ..., $R(u), S(d), R(u), S(d), \dots$ or ..., $R(u), S(d), S(d), R(u), \dots$ or any other combination thereof. Whether the domains formed by the racemic mixture are enantio-pure or not, they would appear as non-superimposable mirror-image symmetries of each other with respect to the property of the clockwise and counter-clockwise LT angles. An STM study of the self-assembly of the pure enantiomers (without the coadsorbate hexadecanoic acid) on graphite has yet to be performed. For such a case, the property of either clockwise or counter-clockwise LT angle morphology for a given enantiomer would unambiguously identify the up or down orientation of the Br atom, in a manner similar to the coadsorbate case discussed above.

The calculations performed in this paper are designed to assess the relative stabilities of the enantio-pure and enantio-mixed formations of racemic mixtures of 2-bromohexadecanoic acid on graphite. We note that the calculations are carried out under the equivalent of vacuum experimental conditions and without image charge interactions with the graphite lattice. The calculations, therefore, serve only as a first-order approximation to the experimentally studied system at the graphite–solvent interface^{15,16} and may underplay some of the important aspects of the interactions of the polarizable bromine atoms with the graphite lattice and the solvent. Nevertheless, the picture of the surface assemblies and their chiral properties developed through these simulations are expected to provide clues concerning the likely results of experiments performed at the vacuum–solid interface, the relative stability of different 2D polymorphic assemblies, and (at least indirectly) the potential for manipulating self-organizing structures through variations in solvent identity for systems assembled at a liquid–solid interface.

Methods

The simulation (SIM) molecular dynamics program (H. A. Stern, H. Xu, E. Harder, F. Rittner, M. Pavese, and B.J.B., unpublished work) was used for all of the calculations described here. The all-atom optimized potentials for liquid simulations (OPLS-AA) force field^{21,22} was employed for the intramolecular and intermolecular interactions of the adsorbate molecules. The intramolecular potential energy consists of harmonic angular bending and bond stretching contributions, and the torsions are modeled by a Fourier expansion in the dihedral angles. The intermolecular interactions are represented by nonpolarizable electrostatics and a standard 6–12 Lennard Jones (LJ) potential to describe van der Waals (vdW) dispersive and repulsive forces. A geometric combining rule is used for the calculation of LJ parameters for unlike atoms. The electrostatic and LJ parameters for the alkyl chains were taken from the standard OPLS-AA parameter files, whereas the halogenated and carboxylic functional was specially fitted by employing the triple- ζ contraction of the Los Alamos LACVP²³ basis set (LACV3P), Becke's three-parameter exchange functional, and the Lee, Yang, and Parr correlation functional (B3LYP)^{24,25} within the Jaguar program²⁶ to extract more exact electrostatics for the head group. The partial charges of the head group were adjusted slightly to interpolate with the standard OPLS-AA values for the partial charges of the carbon and hydrogen atoms of the alkyl tail under the condition for total neutrality. The methodology described here is based on the work done in ref 27 except for the use of the united atom OPLS force field in the original formulation.

In addition, we have not included in this paper image charge interactions due to divergences resulting from the penetration of the atoms of the hydroxyl group into the graphite lattice. This happens because the vdW radii of the oxygen and hydrogen atoms of the hydroxyl group are smaller than the vdW radius of the graphitic carbon atom.

The interaction with the hexagonal graphite substrate is described by the static Steele²⁸ potential. The Steele potential describes the graphite surface by a Fourier expansion in the graphite lattice vectors, and the substrate–adsorbate interactions through a LJ potential. The top 2 layers are modeled as a fully corrugated potential, and the rest of the substrate is included as a smooth potential for a total of 40 layers. The parameters used for the Steele potential ($\sigma_{\text{surface}} = 3.55 \text{ \AA}$, $\epsilon_{\text{surface}} = 0.07 \text{ kcal/mol}$), when used with a geometric combining rule and the standard OPLS alkyl parameters, were found to closely match the previously reported values^{29,30} used to compare calculated and experimental melting temperatures of alkane monolayers on graphite surfaces.

All of the minimizations were performed by using the truncated Newton algorithm package TNPack³¹ within SIM. A large number of minimizations, initiated from simulated annealing runs at temperatures of 5–100 K, were carried out for each system to prevent structures from becoming trapped at local minima on the potential energy surface. Molecular dynamics in SIM were carried out for the NVT ensemble, by using the Nose–Hoover chains method^{32,33} for the proper equilibration of the bath temperature in the canonical ensemble. The simulations are performed without periodic boundary conditions to avoid imposing an artificial periodicity on the system, thereby obtaining an independent validation of the experimentally determined unit cell parameters under vacuum conditions. Such a methodology has been employed by Cheng and Klein, and Krishnan and Balasubramanian for the study of melting³⁴ and registry^{35,36} transitions of ethylene and *n*-hexane, respectively, on graphite. Ideally, the study of morphology transitions should be carried out by a variable box-shape method.³⁷ The application of the Steele potential restricts, however, the lengths of the simulation box to be an integer multiple of the graphite periodicity.

Results

The self-assembly of $(R)/(S)$ -2-bromohexadecanoic acid on graphite was examined in isolation,^{15,16} that is, without the coadsorbate hexadecanoic acid.¹⁷ The racemic system by itself forms well-defined patterns that are more amenable than the coadsorbate mixture to molecular and theoretical modeling. We also believe that the two systems are complementary and that conclusions drawn from one should also be relevant to the other. The analysis is performed by comparing the energetics of the self-assembled morphologies of the enantio-pure and enantio-mixed domains of $(R)/(S)$ -2-bromohexadecanoic acid on graphite. We begin with the former scenario for which the racemic mixture segregates into enantio-pure domains of either (R) -2-bromohexadecanoic acid or (S) -2-bromohexadecanoic acid with all of the bromine atoms pointing either up or down. The energy minimized configurations for the (R) and (S) enantiomers of 2-bromohexadecanoic acid with all of the bromine atoms oriented up are displayed in Figure 2A and B, respectively, for a total of 24 chains. The 50° clockwise (Figure 2A) and 50° counter-clockwise (Figure 2B) LT morphologies are mirror images of each other. The corresponding configurations for the down orientation of the bromine atoms are displayed in Figure 2C and D, respectively. Here the (R) and (S) enantiomers display

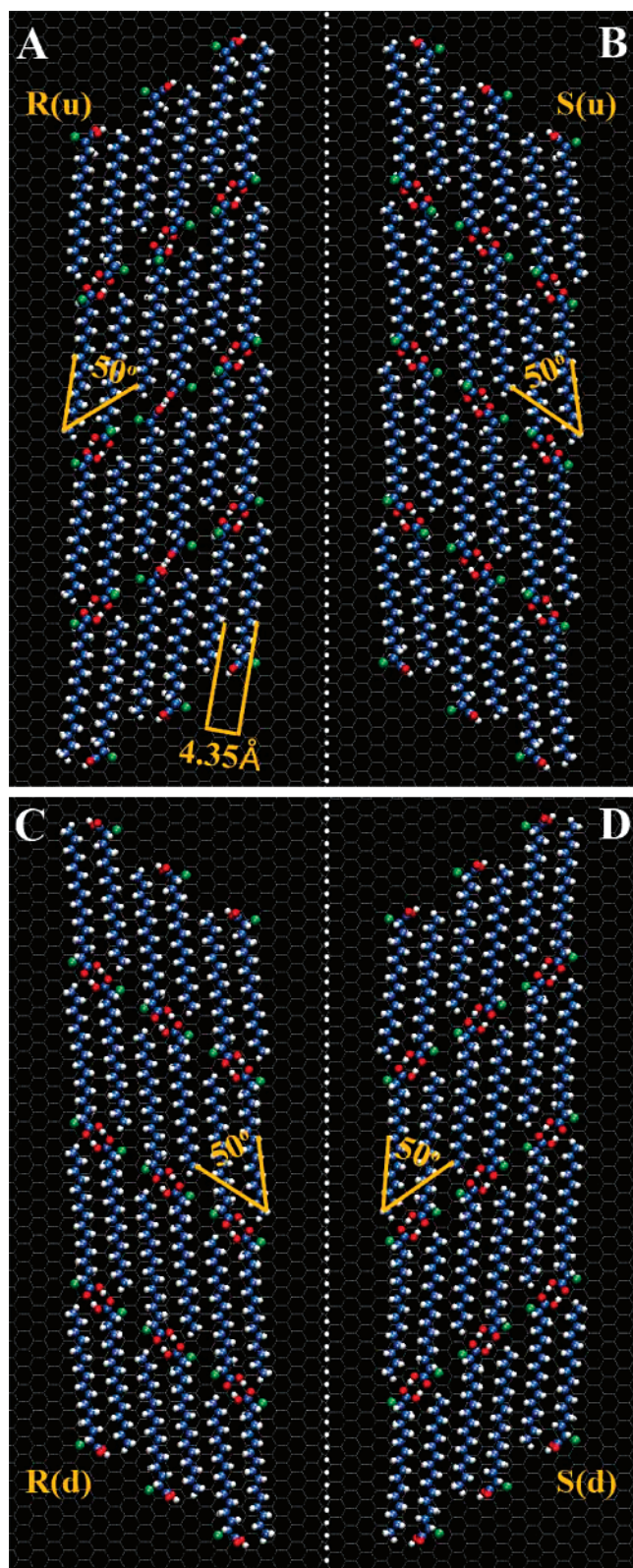


Figure 2. Minimized configurations of enantio-pure domains (top view). $R(u)$ in 2A and $S(u)$ in 2B correspond to the (R) and (S) enantiomers, respectively, with the bromine atoms in the up orientation. Similarly $R(d)$ in 2C and $S(d)$ in 2D correspond to the bromine atoms in the down orientation. The domains on the left and right column are mirror images of each other across the reflection plane indicated by the dashed white line. The carbons, hydrogens, oxygens, and bromines are colored, blue, white, red, and green, respectively. The lamella-trough angle is approximately 50° . The images have been created by VMD.⁴² opposite mirror symmetries (50° counter-clockwise and 50° clockwise LT angles, respectively) relative to the up case.

The counter-clockwise and clockwise mirror symmetries of the LT angle can also be obtained using a mixture of the (R) and (S) enantiomers. Figure 3A, for example, displays an energy minimized 41° counter-clockwise LT angle configuration for the $R(d)/S(u)$ mixture. The enantiomers are ordered along the lamellae as $\dots R(d), S(u), R(d), S(u), \dots$. We have considered this specific ordering because it maximizes the density of hetero-chiral interactions. Figure 3B and C displays the energy-minimized configurations for $R(d)/S(u)$ for two other counter-clockwise LT angles of 47° and 60° , respectively. The enantio-pure and enantio-mixed configurations in Figures 2B and 3B, respectively, display slightly different counter-clockwise LT angles of 50° and 47° , respectively, despite the identical packing of the chains. The LT angle of approximately 50° is in good agreement with experiment.^{15,16} The different configurations in Figure 3A–C were obtained by shifting pairs of columns (along the chain axis) relative to each other by one methylene group. The orange arrows at the bottom right of Figure 3A–C indicate the progressive displacement of the CH_2 units. The columns displace as pairs in order to maintain the hydrogen bonding of the carboxylic head groups.

The average interchain distance at the energy-minimized configurations of 2-bromohexadecanoic acid, 4.35 \AA , (orange arrows in Figure 2A) is approximately the same as that of n -alkanes, suggesting that 2-bromohexadecanoic acid forms close-packed monolayers despite its relatively bulky head group. The configurations were also observed to maintain their close-packed formation at $T = 298 \text{ K}$. Our results and those of STM studies^{19,38} have been confirmed by a recent X-ray and neutron diffraction study³⁹ showing that carboxylic acid molecules self-assemble into close-packed formations with their backbone skeleton parallel to the graphite surface. STM experiments^{15–17} also depict a moiré pattern along the lamellae direction with a periodicity of approximately six chains. The origin of the moiré pattern, according to our calculations, is due to the small dilation of the average interchain distance relative to the corresponding spacing of the graphite lattice, 4.26 \AA , as well as to the systematic tilt of the axis of the chains with respect to the principal vector of the graphite lattice (within the plane of the graphite surface). The systematic tilt, for both the enantio-pure (Figure 2A–D) and the enantio-mixed (Figure 3A–C) morphologies, is due to the diagonal orientation of the hydrogen bonds of the carboxylic groups across neighboring columns. The periodicity, due to the tilt of the chain axis, is depicted, for example, by the top left and bottom right of the diagonal orange line in Figure 3C where the repeating position of the backbone atoms with respect to the graphite lattice takes place. Moiré patterns have also been reported for n -carboxylic acids on graphite with a slightly smaller periodicity of four–five chains.^{38,40}

The energy minimizations of the enantio-pure configurations have been observed to proceed very slowly, suggesting that the configurations in Figure 2A–D may not correspond to the global minimum configurations. The convergence rate could have been improved, in principle, by decreasing the system size. The ratio, however, between the number of “dangling” (edge) carboxyl groups and the number of (inner) “paired” carboxyl groups is already rather large for the 24-chain system. The energy minimizations of the enantio-mixed configurations, however, proceed much faster. Although the enantio-mixed configurations (Figure 3A–C) are likely to be the global minimum configurations, we have decided, nevertheless, to calculate the average potential energy at 5 K (data sampled over 200 ps) of both the enantio-pure and enantio-mixed configurations in order to

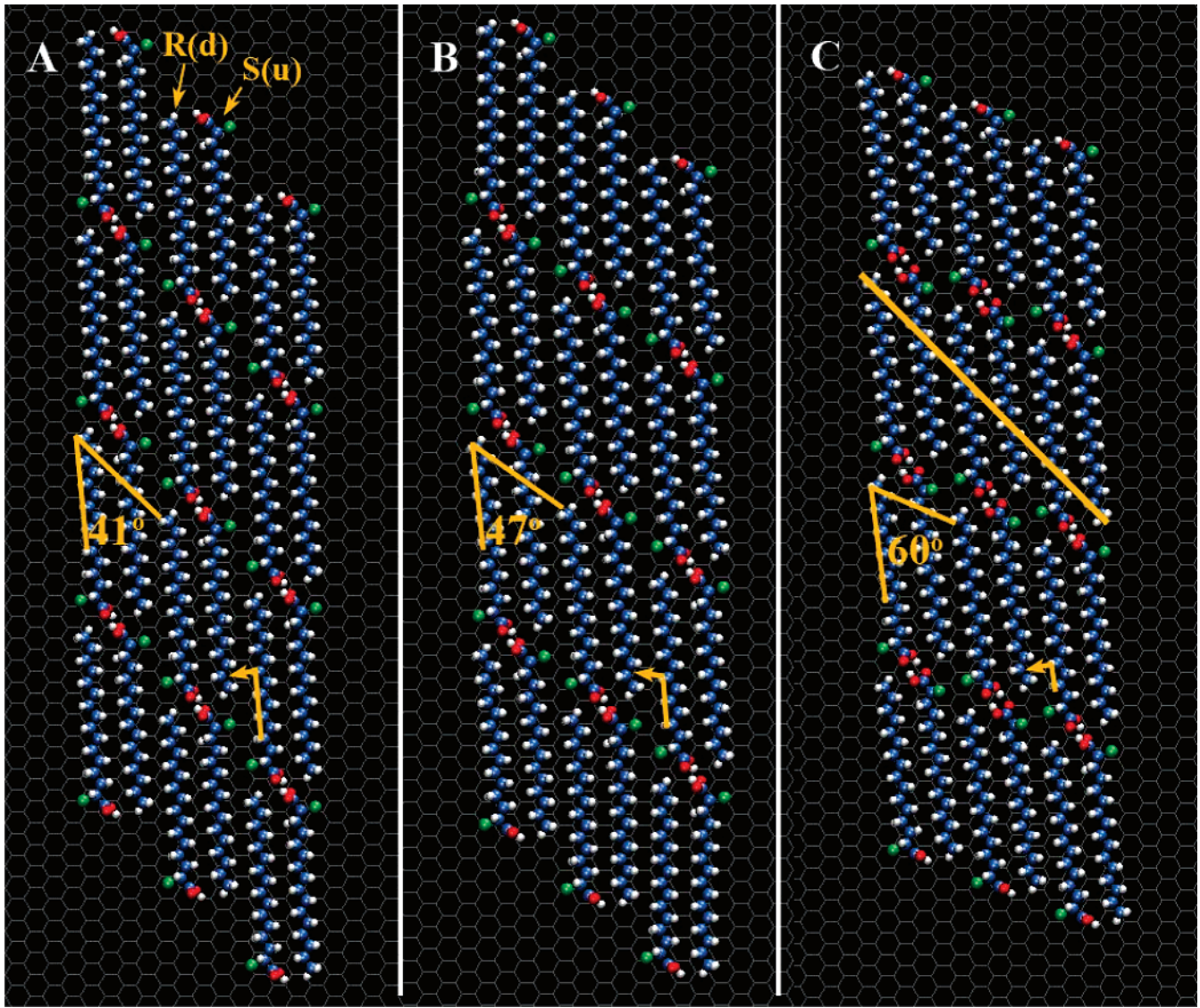


Figure 3. Minimized configurations of enantio-mixed domains formed by pairs of *R(d)/S(u)*-2-bromohexadecaonic acid. *R(d)* corresponds to (*R*) enantiomers with the bromines in the down orientation, and *S(u)* corresponds to (*S*) enantiomers with the bromine atoms in the up orientation. The three configurations, A–C, differ from each other by the lamellae-trough angle, 41°, 47°, and 60°, respectively. The orange line and arrows are discussed in the text.

TABLE 1

	1	2	3	4	5	6	7
kcal/mol/molecule	<i>R(u)</i> 50°	<i>R(d)</i> 50°	<i>R(u)</i> 60°	<i>R(d)</i> 60°	<i>R(d)/S(u)</i> 41°	<i>R(d)/S(u)</i> 47°	<i>R(d)/S(u)</i> 60°
total	−40.5634	−40.4965	−41.2086	−41.0224	−41.8431	−41.8224	−41.9980
stretch	0.9434	0.9999	0.9379	0.9629	0.9419	0.9539	0.9310
bend	3.3133	3.3330	3.2720	3.2684	3.4035	3.3538	3.2029
torsion	2.5430	2.4501	2.5110	2.4641	2.4659	2.4887	2.4382
electrostatic	−6.1078	−5.8738	−6.4532	−6.1465	−6.5662	−6.6954	−6.7323
Lennard-Jones	−6.4036	−5.8649	−6.8616	−6.2994	−6.2830	−6.1636	−6.8029
Steele	−34.8517	−35.5408	−34.6148	−35.2718	−35.8053	−35.7597	−35.0350

compare their energetics. Because the configurations sampled at such a low temperature may also become trapped in a local minimum, we have initiated the sampling from many different simulated annealing runs (more so for the enantio-pure systems) with the aim of exploring the immediate basin of the global minimum configuration.

The breakdown of the average potential energy at 5 K into individual contributions is displayed in Table 1. The up and down 50° clockwise LT angle configurations of the (*R*) enantiomer (Figure 2A and C, respectively) are given in the first and second columns of Table 1, respectively. The corresponding breakdown for the 60° clockwise LT angle (image

not shown) is given in the third and fourth columns of Table 1, respectively. The 41°, 47°, and 60° clockwise LT angles of the *R(d)/S(u)* mixture (Figure 3A–C, respectively) are given in the fifth, sixth, and seventh columns of Table 1, respectively. Although the variation in the energies between the different morphologies (Table 1) is relatively small, it is physically significant because the morphologies differ from each other only by the LT angle and/or the right or left handedness property of the molecules according to the interchange of the positions of the bromine and hydrogen atoms. The majority of the interactions, that is, the interaction of the long fatty acid tails with

each other and the substrate, remain largely the same among the different morphologies.

Table 1 displays several trends. First, we note that the total potential energies of the enantio-pure configurations are only slightly lower for the up versus the down orientations of the Br atoms. The calculations predict therefore that the up orientation is marginally more stable than the down orientation under vacuum conditions. Experimentally, the up orientation has been observed to be stable at the graphite–solvent interface. The small differences between the total potential energies of the up and down configurations of the enantio-pure system arise from an approximate cancellation of the favorable LJ and electrostatic contributions to the up configurations with the favorable Steele contributions to the down configurations. The torsion term also contributes to a small extent to the down configurations.

Interestingly, the potential energies of the enantio-pure configurations are noticeably higher than those of the enantio-mixed *R(d)/S(u)* configurations (this is in addition to the much slower convergence to the global minima for the enantio-pure configurations). Entropy considerations also suggest that the preference for enantio-mixing should increase with temperature (the STM experiments were performed under ambient conditions). The stability of the enantio-mixed system arises from the (exclusive) addition of the favorable LJ and electrostatic contributions for the up orientation and the favorable torsion and Steele contribution for the down orientation. This observation follows from comparison of the enantio-mixed and enantio-pure configurations, corresponding to identical chain packing and (approximately) identical LT angles (column six with columns one and two, and column seven with columns three and four). The enantio-mixed system is therefore enjoying the best of both the up and down worlds. The stability of the enantio-mixed system also correlates with the small variation of its potential energy as a function of the LT angle (columns five, six, and seven) because pairs of up and down enantiomers can more easily establish the hydrogen bonding at the head groups and adjust to variations in the packing of the chains.

2-Bromohexadecaonic acid is an elongated molecule with a (C–Br) dipole moment at the chiral center, which is approximately perpendicular to the principal molecular axis. Such molecules were classified, according to calculations using an integral equation theory of electrically charged hard spheres, to be chirally discriminating.⁸ Chiral discrimination leads strictly to the formation of either enantio-pure or enantio-mixed domains. Our calculations at the graphite–vacuum interface along with the 3D crystallographic data¹⁸ suggest that 2-bromohexadecaonic acid molecules interact favorably with their mirror-image enantiomers, leading to the formation of enantio-mixed domains. The graphite–solvent interface introduces additional considerations by modifying the external field felt by the (up and down) orientations of the C–Br dipole moment, and the equilibrium position of the highly polarizable Br atom. The two enantiomers of 2-bromohexadecanoic acid are also overall geometrically very similar because only the Br and H atoms are exchanged by the mirror-image symmetry operation. This suggests that the approach used here, based on potential energy calculations of putative close-packed configurations from experimental data, is sufficient to assess the strength of the chirally discriminating interactions. Alternatively, it has been shown that molecules with a highly asymmetric chiral center, that do not form close-packed morphologies, should be sampled over a larger region of configuration space according to free-energy-type calculations.⁹

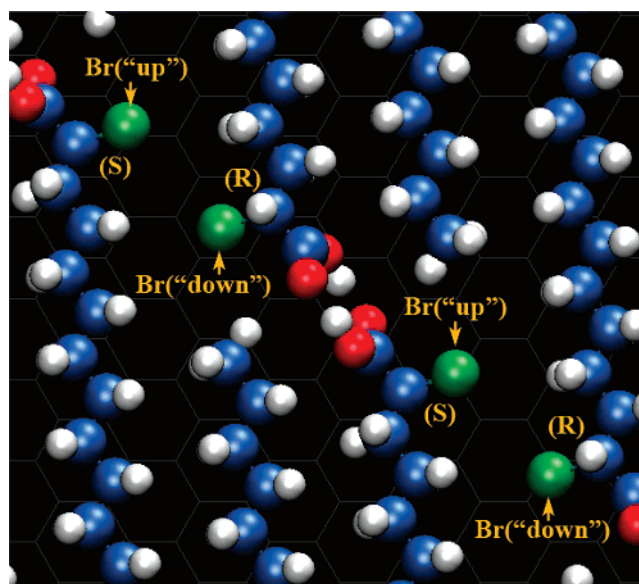


Figure 4. An enlargement of the 47° lamellae-trough angle morphology depicted in Figure 3B. The nearly parallel orientation of the C–Br vector with respect to the graphite surface is seen for both the *S(u)* and *R(d)* enantiomers; the height of the up and down Br atoms above the graphite surface is very similar.

Figure 4 depicts a close-up picture of the enantio-mixed *R(d)/S(u)* system for the 47° LT morphology (enlarged from Figure 3B). The more stable packing and torsion interaction energies of the enantio-mixed system are likely due to the reduced steric hindrance between nearest neighbor pairs of up and down bromine atoms. The more stable electrostatic interactions are probably due to favorable (non-opposing) orientations of the up and down pairs of neighboring C–Br dipole moments. Alternatively, the *x*–*y* projection (onto the graphite plane) of the up and down pairs of the C–Br dipole moments approximately face each other for the 60° LT morphology (Figure 3C); nevertheless, the electrostatic energy of the 60° LT morphology is lower than that of the 47° LT morphology (compare column seven with six in Table 1).

Noticeably, the up and down Br atoms are located at very nearly the same *z*-axis position (vertical direction above the graphite surface). For the 47° LT morphology (Figure 3B), the up and down Br atoms are positioned, on average, at 3.62 Å and 3.35 Å, respectively, above the top layer of graphite atoms. The corresponding hydrogen atoms, right below the up Br atoms and right above the down Br atoms are positioned, on average, at 1.78 Å and 5.31 Å, respectively, above the top graphite layer. The approximately parallel orientation of the C–Br vector (for both the up and down orientations of the Br atoms) with respect to the graphite surface (Figure 4) requires the chains to twist at the expense of increasing the torsion energy. See, for example, the “upward” twisting hydrogen atoms on the methylene group preceding the β carbon for the *S(u)* enantiomer. For the 60° LT morphology (Figure 3C), most of the up and down Br atoms are similarly positioned; however, a few of the up bromines are positioned at a height of 5.8 Å above the top graphite layer; this is due to the larger penalty of the opposing up and down C–Br dipole moments for the 60° LT morphology. The small difference between the height of the up and down Br atoms above the graphite surface is due to the large value of the Lennard-Jones ϵ parameter for Br, which is larger by a factor of approximately 7 and 16 than that of carbon and hydrogen, respectively. This translates into a deep potential well for the

van der Waals dispersion interactions between Br and other atoms, which confines the equilibrium distance of the Br atoms with respect to the fixed atoms of the graphite lattice. The small difference between the heights of the up and down Br atoms above the graphite layer suggests that the lack of apparent variation in the STM image contrast of the Br atoms may not, necessarily, indicate that all of them are orientated up.

Finally, we note that the potential energies of the enantio-pure configurations for both the up and down orientations are lower by more than 0.5 kcal/mol/chain for the 60° LT angle (columns three and four) relative to the (experimentally observed) 50° LT angle (columns one and two). The potential energy of the enantio-mixed configurations is less sensitive to the LT angle (columns five, six, and seven), yet the potential energy of the 60° LT angle arrangement is still lower than that of the (experimentally observed) 47° LT configuration by ~0.18 kcal/mol/chain. The lower potential energy of the 60° LT angle morphology could be accounted for by noticing that it is tightly packed with a maximal overlap between the atoms of neighboring chains. Some of the difference may also be an artifact of the finite boundary conditions because the length of the boundary contour increases with decreasing LT angle. The more compact 60° LT packing geometry may also be surrounded by large barriers in the potential energy surface, suggesting a kinetic origin for the discrepancy between the theoretical prediction for the most stable LT angle morphology and experiment. We also note that all of the configurations and systems studied were generally sensitive to the setup of the initial configuration and that small variations in the relative placement of the chains with respect to each other would often produce configurations with various degrees of long-lived disorders about the ideal packing geometry.

Discussion

The lower potential energy of the enantio-mixed configurations in combination with the much faster minimization of its potential energy strongly suggests that the self-assembled domains of the racemic (*R*)/(*S*)-2-bromohexadecanoic acid, if deposited under vacuum conditions, would not be enantio-pure but rather would form mixtures of either *R*(u)/*S*(d) or *R*(d)/*S*(u) enantiomers. (*R*)/(*S*)-2-Bromohexadecanoic acid is therefore likely to self-assemble under vacuum in accordance with its 3D mode of crystallization.¹⁸ The *R*(u)/*S*(d) and *R*(d)/*S*(u) domains would, under these conditions, contain an equal amount of (*R*) and (*S*) enantiomers. UHV STM studies of self-assembly at the graphite–vacuum interface are clearly feasible based on earlier studies of haloalkanes adsorbed on graphite in vacuum.²⁷ Thus, it should be possible to investigate the self-assembly patterns of a racemic mixture of 2-bromohexadecanoic acid vacuum evaporated onto a graphite surface. Of course, some care must be exercised to guarantee that the lowest energy configuration of the monolayer self-organized structure is reached. Given the relatively high vapor pressure of 2-bromohexadecanoic acid, it should be possible to anneal the initially deposited films in order to reach the thermodynamically most stable structure.

Even though the omission of both solvent effects and image charge interactions is a significant approximation for the question at hand, our calculations suggest a competition between the intrinsic stability that results from mixing pairs of up and down enantiomers of opposite mirror symmetry and the stability of the up orientation of the Br atoms at the graphite–solvent interface. The enantio-mixed pairs enjoy the best of both the up and down worlds. The enantio-identity of the domains formed

by racemic (*R*)/(*S*)-2-bromohexadecanoic acid at the graphite–solvent interface, either by itself or coadsorbed with hexadecanoic acid, depends, therefore, on the strength of the solvent induced stabilization of the up orientation of the Br atoms relative to the stability gained by mixing pairs of up and down enantiomers of opposite mirror symmetry. Inclusion of an image charge contribution is expected to stabilize the down orientation of the Br atoms, whereas inclusion of explicit solvent molecules is expected to stabilize the up orientation. The capping solvent molecules would predominantly interact with the up-oriented Br atoms through both dispersion forces and dipole-induced configurational reorganization. The image charge contribution, however, reflects the response of the conduction electrons of the graphite lattice to the charge distribution of the adsorbate (and solvent) layers. The dispersive interaction of the adsorbate layer with the graphite lattice is already accounted for through the Steele (LJ) contribution.

We note that the STM images of the racemic (*R*)/(*S*)-2-bromohexadecanoic acid at the graphite–solvent interface do not appear to reveal any strong variation in the contrast between adjacent atoms of the bromine dimers^{15–17} in support of the assumption that the domains are enantio-pure with all of the bromine atoms oriented up. Alternatively, the calculations also suggest that the difference in height above the graphite surface for the two Br atoms of an *R*(d)/*S*(u) dimer pair is quite small (~0.3 Å). In addition, the electrical interaction of the two up and down Br atoms with the surface will be slightly different, which is likely to cause a variation in the local density of states near the graphite Fermi level sensed by the STM. Taken together, these effects could lead to similar STM contrast for up and down Br atoms of a given dimer pair. This issue may be resolved by studying the self-assembly of pure *R*- and/or *S*-2-bromohexadecanoic acid at the phenyloctane/graphite interface using STM. The unambiguous assignment of the up orientation of the bromine atoms for the self-assembly of the pure enantiomers of 2-bromohexadecanoic acid (with the coadsorbate hexadecanoic acid) at the graphite–solvent interface¹² also suggests the importance of incorporating solvent effects and image charge interactions to properly model the interfacial environment experienced by the highly polarizable bromine atom. Recent studies of self-assembly of trimesic acid have shown the importance of solvent effects in determining the stability of different 2D polymorphic surface structures.⁴¹ Our calculations indicate that further lessons can also be learned by performing the same self-assembly experiments under vacuum conditions as well as under solvents with different structural and electrostatic properties.

Acknowledgment. We thank Harry A. Stern and Tova L. Werblowsky for sharing with us the SIM computational framework for the study of self-assembly on graphite. This work was supported by the National Science Foundation under grants CHE-06-13401 (to B.J.B.) and CHE-03-52582 (to G.W.F.).

References and Notes

- Attard, G. A. *J. Phys. Chem. B* **2001**, *105*, 3158–3167.
- Jacoby, M. *Chem. Eng. News* **2004**, *82*, 37–41.
- Vidal, F.; Delvigne, E.; Stepanow, S.; Lin, N.; Barth, J. V.; Kern, K. *J. Am. Chem. Soc.* **2005**, *127*, 10101–10106.
- De Feyter, S.; De Schryver, F. C. *Chem. Soc. Rev.* **2003**, *32*, 393–393.
- De Feyter, S.; Uji-i, H.; Mamdoui, W.; Miura, A.; Zhang, J.; Jonkheijm, P.; Schenning, A.; Meijer, E. W.; Chen, Z.; Wurthner, F.; Schuurmans, N.; van Esch, J.; Feringa, B. L.; Dulcey, A. E.; Percec, V.; De Schryver, F. C. *Int. J. Nanotechnol.* **2006**, *3*, 462–479.
- Ernst, K. H. *Supramolecular Surface Chirality*. In *Supramolecular Chirality*; Springer: New York, 2006; Vol. 265, pp 209–252.

- (7) Humblot, V.; Barlow, S. M.; Raval, R. *Prog. Surf. Sci.* **2004**, *76*, 1–19.
- (8) Paci, I.; Cann, N. M. *J. Chem. Phys.* **2004**, *120*, 4816–4828.
- (9) Paci, I.; Szleifer, I.; Ratner, M. A. *J. Am. Chem. Soc.* **2007**, *129*, 3545–3555.
- (10) Hermse, C. G. M.; van Bavel, A. P.; Jansen, A. P. J.; Barbosa, L.; Sautet, P.; van Santen, R. A. *J. Phys. Chem. B* **2004**, *108*, 11035–11043.
- (11) Bohringer, M.; Morgenstern, K.; Schneider, W. D.; Berndt, R.; Mauri, F.; De Vita, A.; Car, R. *Phys. Rev. Lett.* **1999**, *83*, 324–327.
- (12) Yablon, D. G.; Guo, J. S.; Knapp, D.; Fang, H. B.; Flynn, G. W. *J. Phys. Chem. B* **2001**, *105*, 4313–4316.
- (13) Cyr, D. M.; Venkataraman, B.; Flynn, G. W.; Black, A.; Whitesides, G. M. *J. Phys. Chem.* **1996**, *100*, 13747–13759.
- (14) Faglioni, F.; Claypool, C. L.; Lewis, N. S.; Goddard, W. A. *J. Phys. Chem. B* **1997**, *101*, 5996–6020.
- (15) Fang, H. B.; Giancarlo, L. C.; Flynn, G. W. *J. Phys. Chem. B* **1998**, *102*, 7311–7315.
- (16) Fang, H. B.; Giancarlo, L. C.; Flynn, G. W. *J. Phys. Chem. B* **1999**, *103*, 5712–5715.
- (17) Yablon, D. G.; Giancarlo, L. C.; Flynn, G. W. *J. Phys. Chem. B* **2000**, *104*, 7627–7635.
- (18) Parkin, G. X-ray crystallography of purified (*R*)/(*S*)-2-bromohexadecanoic acid revealed crystals composed of both enantiomers bonded together. Personal communication.
- (19) Hibino, M.; Sumi, A.; Tsuchiya, H.; Hatta, I. *J. Phys. Chem. B* **1998**, *102*, 4544–4547.
- (20) Giancarlo, L. C.; Flynn, G. W. *Acc. Chem. Res.* **2000**, *33*, 491–501.
- (21) Jorgensen, W. L. *J. Phys. Chem.* **1986**, *90*, 1276–1284.
- (22) Udier-Blagovic, M.; De Tirado, P. M.; Pearlman, S. A.; Jorgensen, W. L. *J. Comput. Chem.* **2004**, *25*, 1322–1332.
- (23) Hay, P. J.; Wadt, W. R. *J. Chem. Phys.* **1985**, *82*, 299–310.
- (24) Becke, A. D. *J. Chem. Phys.* **1993**, *98*, 5648–5652.
- (25) Lee, C. T.; Yang, W. T.; Parr, R. G. *Phys. Rev. B* **1988**, *37*, 785–789.
- (26) *Jaguar 6.5*; Schrödinger, LLC: New York, 2005.
- (27) Muller, T.; Werblowsky, T. L.; Florio, G. M.; Berne, B. J.; Flynn, G. W. *Proc. Natl. Acad. Sci. U.S.A.* **2005**, *102*, 5315–5322.
- (28) Steele, W. A. *Surf. Sci.* **1973**, *36*, 317–352.
- (29) Peters, G. H.; Velasco, E. *Mol. Phys.* **1995**, *84*, 1039–1047.
- (30) Velasco, E.; Peters, G. H. *J. Chem. Phys.* **1995**, *102*, 1098–1099.
- (31) Schlick, T.; Fogelson, A. *AcM Transactions on Mathematical Software* **1992**, *18*, 46–70.
- (32) Martyna, G. J.; Klein, M. L.; Tuckerman, M. *J. Chem. Phys.* **1992**, *97*, 2635–2643.
- (33) Nose, S. *J. Chem. Phys.* **1984**, *81*, 511–519.
- (34) Cheng, A.; Klein, M. L. *Langmuir* **1992**, *8*, 2798–2803.
- (35) Krishnan, M.; Balasubramanian, S.; Clarke, S. *Proc. Indian Acad. Sci., Chem. Sci.* **2003**, *115*, 663–677.
- (36) Krishnan, M.; Balasubramanian, S.; Clarke, S. *J. Chem. Phys.* **2003**, *118*, 5082–5086.
- (37) Parrinello, M.; Rahman, A. *J. Appl. Phys.* **1981**, *52*, 7182–7190.
- (38) Hibino, M.; Sumi, A.; Hatta, I. *Jpn. J. Appl. Phys., Part 1* **1995**, *34*, 3354–3359.
- (39) Bickerstaffe, A. K.; Cheah, N. P.; Clarke, S. M.; Parker, J. E.; Perdigon, A.; Messe, L.; Inaba, A. *J. Phys. Chem. B* **2006**, *110*, 5570–5575.
- (40) Hibino, M.; Sumi, A.; Hatta, I. *Jpn. J. Appl. Phys., Part 1* **1995**, *34*, 610–614.
- (41) Lackinger, M.; Griessl, S.; Heckl, W. A.; Hietschold, M.; Flynn, G. W. *Langmuir* **2005**, *21*, 4984–4988.
- (42) Humphrey, W.; Dalke, A.; Schulten, K. *J. Mol. Graphics* **1996**, *14* (1), 33–&.